An Application of Laser Diagnostics to the Study of End-Gas Autoignition and Engine Knock

R.M. Green and R.P. Lucht
Combustion Research Facility
Sandia National Laboratories
Livermore, CA 94550

ABSTRACT

Stable and repeatable knocking operation has been achieved in a spark ignition, optical research engine. High swirl and multipoint ignition are used to confine the end gas in the center of the combustion chamber, while manifold temperature and pressure control the degree of the knock response. Knock appears to be the result of a nearly homogeneous and simultaneous autoignition of the end gas.

Two laser diagnostic techniques, spontaneous Raman scattering and coherent anti-Stokes Raman spectroscopy (CARS), were used to measure the end-gas temperature history. These techniques are described and the results are compared. Higher end-gas temperatures under knocking conditions are shown to be due to higher wall temperatures.

INTRODUCTION

Engine knock, which can lead to severe engine damage, results from the pressure waves generated by the explosive combustion of the last burned portion of the intake charge (or end gas). This rapid combustion is due to a mechanism which is different from the normal mode of flame propagation. Although for many years there was much disagreement as to the nature of this mechanism, it is now commonly accepted that end-gas autoignition is responsible for the accelerated heat release rate which leads to knock.

For many years the problem of engine knock was adequately controlled by the addition of tetraethyl lead to the fuel. Consequently, little effort was directed toward understanding the underlying fundamental phenomena. When emission standards severely curtailed the use of lead in gasoline, engine designers and fuel producers had to resort to other methods of preventing knock. Lower compression ratios, ignition control systems, complex means of fuel-air preparation, and expensive fuel refining and blending techniques have been satisfactory, at least in the short term, for controlling knock in engines. However, further improvements in fuel economy and performance may require an increase in compression ratio which is now limited by the onset of knock.

Two classes of phenomena govern the autoignition process. First are the fluid and thermal transport processes, which are strongly coupled to the specific characteristics of the engine; second is the chemistry of low-temperature oxidation of the fuel, which is less dependent on engine design. Our current research on engine knock focuses on the latter process. Specifically, our goal is to gain a comprehensive understanding of the low-temperature chemistry that occurs in the compressively-heated end gas prior to the onset of autoignition (1).

The major link coupling experimental observations and measurements to the detailed kinetic modeling of the chemical processes occurring in the end gas is the gas phase temperature. Because of this, a significant portion of our experimental research has been devoted to the measurement of the end-gas temperature history prior to the autoignition event. Here we describe our approach to these measurements.

Measurement of the gas temperature in a knocking engine is not a new objective. A half a century ago Rassweiler and Withrow (2) described the in-cylinder measurement of gas temperatures under both knocking and nonknocking conditions. Using the sodium-line-reversal technique, they made time-resolved, line-of-sight temperature measurements in postflame gases at various positions in the combustion chamber. Their results illustrated the temperature gradient caused by the adiabatic-compression heating of the first-burned gases and, in addition, indicated that under knocking conditions, both the peak temperature and the rate of heat transfer from the combustion chamber were higher than those under nonknocking conditions. Although these measurements did not include the end-gas temperatures, they did pioneer a path for future research.

More recently, there have been a number of studies of autoignition chemistry in an engine (3,4), including the classic work by Downs, Walsh and Wheeler (5). In all this work, researchers investigated end-gas chemistry in detail, using technology that was state of the art for the time. However, none of the results were correlated to an end-gas temperature history. Some investigators did, however, estimate the end-gas temperature history using the cylinder pressure and an assumed gas law, and related that result to the findings of their chemical analyses (6,7). This procedure provided a firmer foundation for their conclusions about the end-gas chemistry, but in-cylinder measurements of the temperature were clearly needed.

In 1961, Gluckstein and Walcutt (8) devised a novel technique to measure the end-gas temperature. They constrained the end gas to a region of the cylinder where a measurement of the local speed of sound could be used to infer the temperature prior to autoignition. These data were used to relate the knocking characteristics of various fuels to the in-cylinder

pressure and temperature histories. Recently, Johnson, Myers and Uyehara (9) performed a similar study using an infrared pyrometer to measure the end-gas temperature along an optical line of sight. These results, along with pressure histories, were used to compute the rate and the extent of chemical energy release, which were then correlated with a simple chemical kinetic model.

Currently available, laser-diagnostic technology now allows us to significantly improve upon past research. High spatial resolution and better temporal resolution allow us to probe the end-gas region up to the time of autoignition, with improved measurement accuracy. This technology, along with a knock research facility in which the end-gas conditions can be carefully established and maintained, should allow us to advance our understanding of the end-gas autoignition phenomenon. In the following sections, we describe our optical research engine and the procedures used to achieve controllable knocking operation. We discuss the operating conditions involved in these experiments, and the nature of the observed knocking response. We also describe how we applied the two techniques used to measure the end-gas temperature history--spontaneous Raman scattering and coherent anti-Stokes Raman spectroscopy (CARS)--and present the measurements obtained. Finally, we discuss those results in terms of the advantages and shortcomings of the techniques.

EXPERIMENT DESCRIPTION

Since in a production engine, end-gas autoignition and knock are both spatially and temporally random, it was important to devise an experimental strategy in which the knock phenomenon is controlled in a stable and repeatable manner. This strategy is especially critical here, because the laser diagnostic measurements are temporally and spatially resolved and also represent an average over an ensemble of engine cycles.

The experiments described in this study were performed using the Sandia optical research engine (10). Radially actuated valves, located in the side wall of the disk-shaped combustion chamber, allow full optical access to the combustion chamber along a direction parallel to the cylinder axis. Two small windows, diametrically opposed in the chamber wall, provide optical access along a direction normal to the cylinder axis. This combustion chamber configuration results in a compression ratio of 5.1:1.

A combination of high-swirl and multipoint ignition confines the end gas to the center of the combustion chamber. A swirl number of 8.3 at TDC is produced by a shrouded intake valve. Normal flame propagation is initiated by four spark plugs equally spaced around the perimeter of the combustion chamber and fired simultaneously. The propagation of the four flame fronts is dominated by swirl-induced convection and confines the end gas in the center of the combustion chamber (illustrated in the schlieren photograph on the left side of Fig. 1). Since only small regions of the piston dome and top window directly contact the end gas, the total heat transfer to the combustion chamber surface is small. In addition, the high turbulence level of this engine leads to good mixing and a reduction of spatial gradients. Both of these factors result in substantially uniform conditions within the end gas, a necessary condition for controlled and cyclically-repeatable chemical reactions.

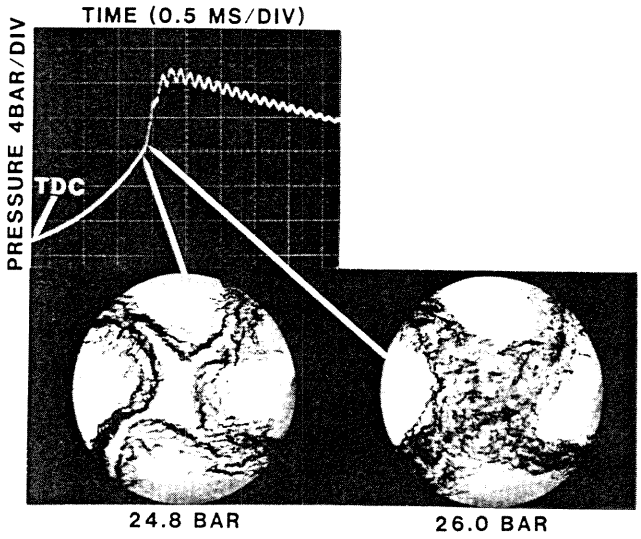

Fig. 1 Schlieren photos of the end-gas region 0.05 ms before and after the autoignition time (knock point). The photos are referenced to the engine cycle using the pressure history during the heat release. Operating conditions: fuel, n-butane;equivalence ratio, stoichiometric; engine speed, 600 RPM; manifold conditions 433 K and 1.53 atm; ignition at TDC.

A low compression ratio leads to a large residual gas fraction from the previous engine cycle, resulting in a high level of cyclic variation. To reduce the cyclic variation, we fire the engine every third cycle, thus lowering the residual fraction of burnt gases to less than 1 percent on the firing cycle. Additionally, a very fast burn of less than 20 crank angle degrees (CAD) also tends to reduce the level of cyclic variation. Preheating and pressurizing the fuel-air mixture in the intake manifold enabled us to obtain knock even with the low compression ratio of our engine. In addition to increasing the effective compression ratio, the control of the manifold conditions allowed us to control the degree of knock response (i.e., the fraction of the fuel-air mixture which autoignited).

PROCEDURE

The knock response of our research engine is caused by a nearly homogeneous and simultaneous autoignition in the end gas. Figure 1 shows a typical combustion chamber pressure history and a pair of schlieren photographs of the autoignition event. The pressure trace covers the time interval from ignition at TDC to well after peak pressure. From the start of heat release, the pressure increases smoothly as the flame fronts propagate normally; this process continues until there is a sudden increase in the rate of pressure rise. This sudden increase is the time of autoignition which we will refer to as the "knock point". Following autoignition, peak pressure is rapidly reached due to the very high rate of heat release, and the pressure trace exhibits the characteristic knock oscillation at a frequency of about 7.5 kHz. This pressure oscillation is driven by the nonuniform pressure distribution in the chamber, caused by the very rapid rate of heat release after

autoignition. The observed frequency corresponds to the transit of a strong acoustic wave or a weak shock from the center of the chamber to the cylinder wall and back. These observations are consistent with those made in production-type engines, with one exception: here, knock occurs earlier in the heat release interval (at about the 60 percent mass-fraction-burned point).

The schlieren photos shown in Fig. 1 correspond to 0.05 ms before and after the knock point. The dark regions represent high spatial gradients of index of refraction (or density); the light regions represent areas of nearly uniform conditions. In the preknock photo, the end gas is confined in the center of the combustion chamber by the propagating flame fronts. The hot postflame gases are the light areas between the cylinder wall and the flame fronts. Although the appearance of the postflame gases and the flame fronts has changed very little in the postknock photo, autoignition has significantly changed the end gas region, which is now burning throughout. Furthermore, the dark, mottled nature of the schlieren image of this region indicates that density gradients exist, implying some inhomogeneity. We have not yet been able to photograph autoignition when only a portion of the end-gas region has autoignited. This would seem to indicate that the autoignition process occurs nearly simultaneously over the whole region.

Operation under knocking conditions can be easily controlled, is very stable, and exhibits excellent cycle-to-cycle repeatability. Depending on the fuel, the operating conditions can be adjusted over a range of knock intensities from incipient knock where only a small quantity of the end gas autoignites, to heavy knock where as much as 80 percent of the initial charge autoignites. For the temperature measurements reported here, the engine was fueled with n-butane at a stoichiometric equivalence ratio, at an engine speed of 600 RPM, and with ignition at TDC. At an intake manifold temperature and pressure of 433 K and 1.53 atm, autoignition occurred 3.2 ms after spark ignition with about 40 percent of initial charge autoigniting. For the end-gas temperature measurements in nonknocking operation, the same operating parameters were used except the manifold pressure was reduced to 1.25 atm.

SPONTANEOUS RAMAN TEMPERATURE MEASUREMENTS

We measured the end-gas temperature history using spontaneous Raman scattering under both knocking and nonknocking conditions. Figure 2 shows the layout of the optical system. The beam of the pulsed Nd:YAG laser was focused at the center of the chamber through the 1.0 cm side windows. The laser could be fired either phase-locked to crankangle or at a preset cylinder pressure. The second harmonic frequency (output at 532.1 nm) of the YAG laser was used at an energy on the order of 75 mJ/pulse. This energy level was limited by the necessity of avoiding window damage or gas breakdown at the focal volume. In order to operate at this level, we had to induce severe spherical aberations in the probe laser beam to soften its focus. We estimate that the resulting scattering volume was about 200 microns in diameter by 1 mm long.

The scattered light was collected through the top window at a 90 degree angle from the probe beam axis and was focused on the entrance slit of a 1/2 meter, single-grating monochromator. The resulting Raman spectrum was detected on an intensified linear diode array and stored on a minicomputer. The spectral dispersion was 1.0 cm^{-1}/pixel or 39.9 cm^{-1}/mm

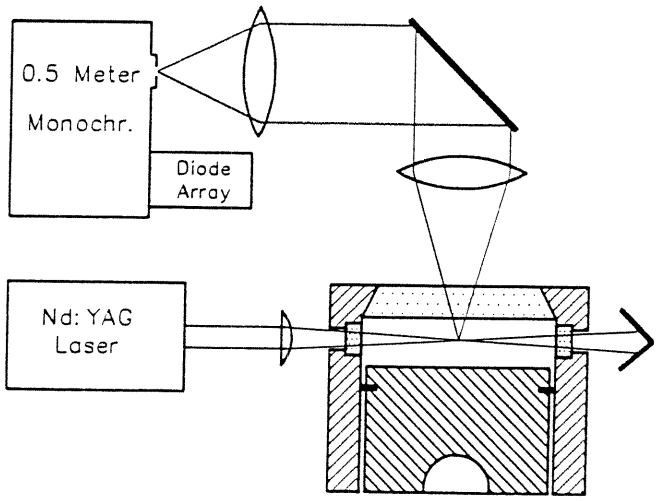

Fig. 2 Schematic diagram of the optical layout of the spontaneous Raman scattering system.

and the slit function had a FWHM of 6.0 pixels. The use of a 20 ns intensifier gating interval eliminates any background light due to flame emission. Since spontaneous Raman has such a small scattering cross section, it was necessary to integrate the signal on the face of the detector for many engine cycles in order to achieve a reasonable signal-to-noise level. For these measurements, 750 engine firing cycles were needed. Since this many cycles requires about 7.5 minutes, considerable dark noise was also accumulated on the detector. Thus it was necessary to correct the Raman signal by subtracting a "dark background"- a spectrum collected under identical conditions except with a closed monochromator entrance slit.

The gas temperature is determined by a theoretical fit of the experimentally obtained spectra using the temperature as a fitting parameter (11). The vibrational Q-branch Raman spectrum of nitrogen is used for most flame temperature measurements (12) because nitrogen is present in high concentrations and its Q-branch Raman spectrum is well-studied spectroscopically. Typical fits are illustrated in Fig. 3. The various peaks represent bands of the vibrational Q-branch. The rightmost peak corresponds to the ground vibrational state, and the peaks lying to the left are due to the excited vibrational states (the energy level increasing with decreasing wavenumber shift).

The result of fitting vibrational Q-branch spectra is essentially the relative populations of the various energy states. This fitting technique is most accurate at higher temperatures, where the excited vibrational energy levels are more populated and the spectrum shows a higher degree of modulation because of the different peaks. The effect of temperature on the spectral modulation is illustrated in Fig. 3. Notice that at a temperature of about 1000 K, the first excited state is practically unpopulated; nearly all the molecules are in the ground state. On the other hand, at 2200 K, three excited states are populated, some to a significant degree. Over the temperature range of compressively heated end gas (700 K to 1100 K), the problem of fitting the data accurately is acute.

It is possible to improve the accuracy of fitting low temperature Raman spectra by using the third har-

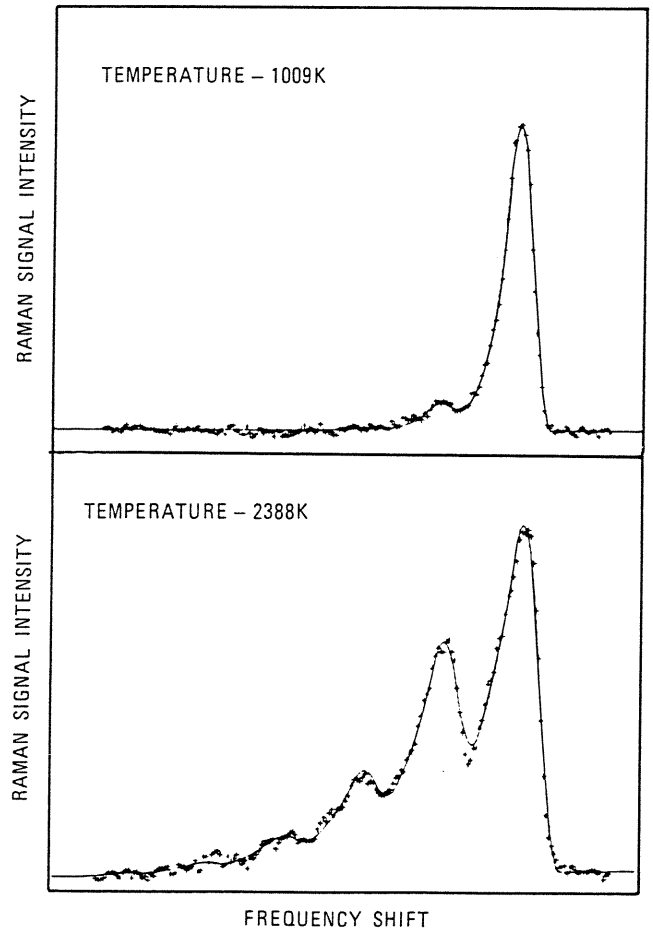

Fig. 3 The spontaneous Raman spectra of nitrogen, obtained in the engine a) at relatively low temperature, where most molecules are in the vibrational ground-state band (top); b) and at higher temperature, where four excited vibrational states are populated, some to a significant degree (bottom).

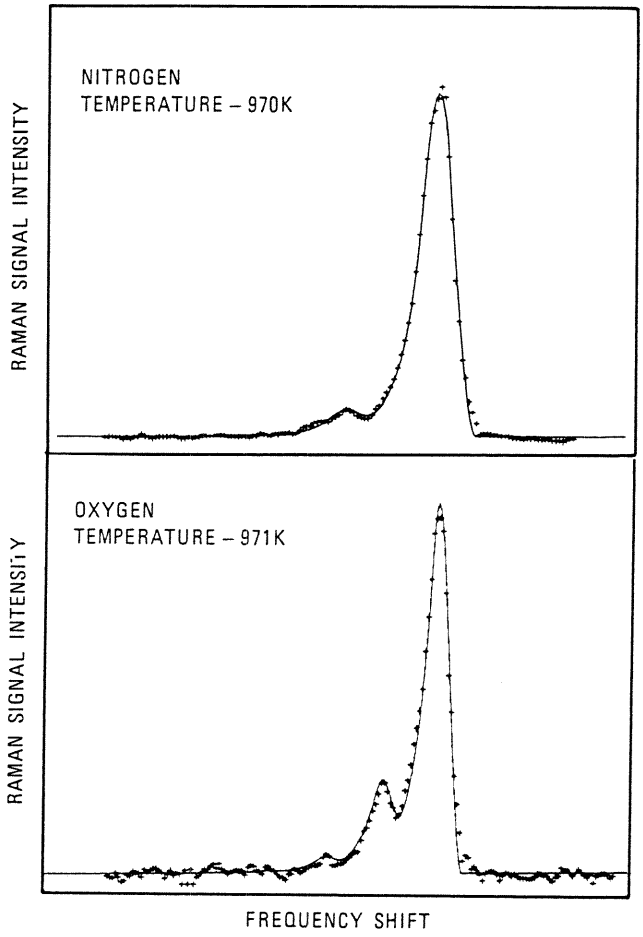

Fig. 4 Spontaneous Raman spectra obtained in the end gas under nonknocking conditions. At the 75% mass fraction burned point (pressure=25 atm), a) the nitrogen spectrum shows one very weak excited state band (top); b) and the oxygen spectrum has two excited states populated (bottom). Notice the difference in the spectral spacing of the vibrational bands between oxygen and nitrogen.

monic (at 354.7 nm) of the YAG output. The fourth-power dependence of the Raman cross section on frequency, results in a factor-of-5 improvement over the signal generated by second harmonic stimulation, and a significant improvement in signal-to-noise ratio can be realized. A further enhancement in the fitting accuracy can be obtained using the Raman scattering from oxygen. The temperature sensitivity of oxygen spectra is higher than that of nitrogen because the energy difference between vibrational levels is smaller, resulting in more populated excited vibrational states at moderate temperatures. This difference is illustrated in Fig. 4 where the Raman spectra of oxygen and nitrogen obtained under identical conditions are displayed. Notice that the peak of the first excited vibrational level is stronger for oxygen than for nitrogen at the same gas temperature, indicating a higher population. In addition, the smaller energy difference between vibrational states is clearly illustrated by the spectral separation between the peaks of the ground and first excited states.

Unfortunately, under knocking conditions, a strong laser-induced fluorescence signal seriously deteriorated the Raman signal-to-noise level. An investigation of the LIF spectrum revealed that it was due to formaldehyde molecules, which are created by low-temperature reactions occurring in the end gas. This condition forced us to use the second harmonic output of the YAG laser. Furthermore, since the oxygen Raman signal stimulated by the YAG second harmonic was so weak, we had to use nitrogen as the scattering medium because of its higher concentration.

Operating under these conditions we observed no LIF; however, we were faced with the problem of fitting low-temperature nitrogen spectra, which exhibit only weak hot bands. Thus, it was necessary to accurately fit the unresolved rotational structure of the ground-state band in order to determine the temperature. Figure 5 illustrates the results of fitting a typical nitrogen Raman spectrum obtained in the end gas. The symbols represent the experimental data points, and the solid line indicates the theoretical fit. The predicted spectrum is an excellent representation of the experimental ground state peak. The fit is especially good in the wings of the band, which are quite sensitive to the temperature. Although

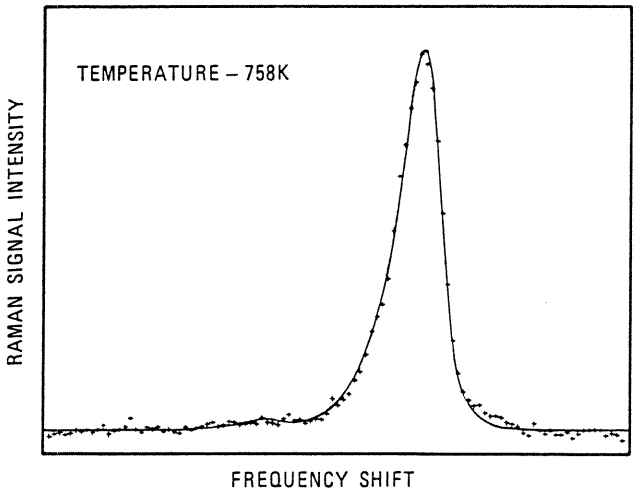

Fig. 5 Typical spontaneous Raman spectrum of nitrogen obtained in the end gas under knocking conditions. The points are the experimental data and the solid line is the theoretical data fit. This spectrum corresponds to the time of spark ignition at TDC.

both the experimental data and the theoretical spectrum exhibit a first excited state, it is so weak that it has little effect on the temperature obtained by the fit. We have determined that this fit of the ground-state peak results in temperature estimates which are accurate to ±75 K.

CARS TEMPERATURE MEASUREMENTS

End-gas temperatures were also measured using CARS from nitrogen. Since in general, a CARS signal is significantly stronger than a spontaneous Raman signal under similar conditions, the data can be gathered at higher resolution, using far fewer engine cycles. The higher spectral resolution of the CARS data improves the temperature-measurement accuracy at lower temperatures. Although this technique has been used previously to measure temperatures in IC engines (13-17), none of this work emphasized the end-gas temperature history prior to autoignition and knock.

In the CARS technique, two laser beams, the pump and the Stokes beams, are focused to a common probe volume. When the frequency difference between the pump and Stokes beams is resonant with a Raman transition, a strong coherent signal at the anti-Stokes frequency is generated. The resonant signal strength is proportional to the square of the population difference between the lower and upper levels of the Raman transition. In addition, a nearly frequency-independent nonresonant CARS signal is generated by the interaction of the laser beams with all molecules in the probe volume. The CARS detection limit is reached when the resonant signal can no longer be distinguished from the nonresonant signal.

The experimental system is illustrated schematically in Fig. 6. The second harmonic frequency of the Nd:YAG laser was used as the CARS pump beam as well as a pumping source for the dye laser, which provided the CARS Stokes beam. The dye laser consisted of a transversely pumped oscillator and an axially pumped amplifier and was operated in a broadband-output configuration, which allows the acquisition of the entire CARS spectrum on each laser shot. The dye laser output was centered around 607 nm by using Rhodamine 640 dye. The central lasing wavelength was fine tuned by adding base or acid to the oscillator dye solution.

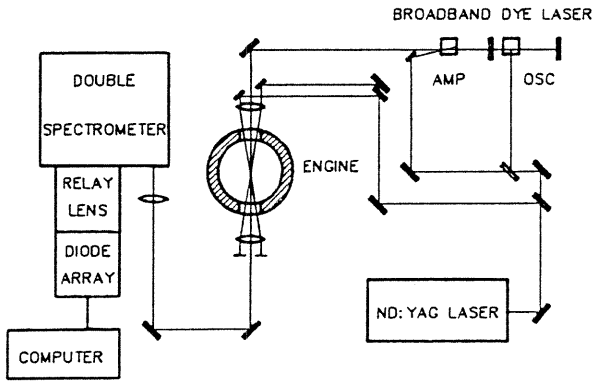

Fig. 6 Schematic diagram of the optical layout of the coherent anti-Stokes Raman scattering system.

The pump and Stokes beams were focused to a common probe volume inside the engine. In this work, laser pulse energies were limited to 5 mJ per beam by gas breakdown in the end gas just prior to knock. Three-dimensional phase matching was used to minimize the interaction length of the pump and Stokes beams and provide better spatial resolution than the colinear (13,17) or near-colinear phase matching schemes (14) used in previous engine experiments. Unfortunately, this technique is more susceptible to beam steering effects because the beams traverse different paths through the engine.

The CARS signal exited the engine spatially separated from the pump and Stokes beams and was focused onto the entrance slit of a double grating spectrometer. A relay lens system was used to magnify and focus the spectrometer image plane onto the face of an intensified linear diode array detector. The spectral dispersion was 5.44 cm^{-1}/mm and the diode array instrument function had a FWHM of 5.5 pixels. The overall resolution of the CARS measurements was 0.75 cm^{-1}. Bothcycle-averaged and single-shot spectra were obtained. As expected, the single shot data were considerably noisier than the cycle-averaged data and will not be reported here.

The nitrogen CARS spectra were normalized by an averaged nonresonant background spectrum obtained both before and after the CARS data. These spectra were acquired with the engine cylinder filled with argon or butane. Drift and noise in the dye laser spectrum were periodically assessed by normalizing a particular nonresonant spectrum by another nonresonant spectrum. If the dye laser output did not drift and was noise-free, the result would be a horizontal, straight line. The actual results show considerable scatter around a least-squares fit, with standard deviations of approximately 20 percent for single shot spectra. The straight lines obtained by normalizing averaged spectra taken before and after the CARS data, showed slopes of approximately 10 percent over the spectral range covered by the first three vibrational Raman transitions of nitrogen.

Gas temperatures were determined by fitting a theoretical nitrogen CARS spectrum to the experimental data. The theoretical spectra were calculated using a recently developed procedure for the efficient calculation of collisional narrowing effects (18). Hall,

Verdieck and Eckbreth (19) showed these effects to be important in the calculation of high-pressure nitrogen spectra. The problem has also been addressed by Hall and Greenhalgh (20) and Kataoka, Maeda, Hirose and Kajiyama (15). One difficulty with earlier treatments of collisional narrowing is that a matrix inversion, required at each frequency point in the spectrum, makes the computation intractable when realistic collisional transfer models are included in the analysis. Koszykowski, Farrow and Palmer (18) transformed the CARS susceptibility equations so that only a single matrix inversion is required to calculate a collisionally-narrowed spectrum. They incorporated an exponential gap collisional transfer model in their analysis and verified their results by comparing the calculated spectra with high pressure CARS data obtained with high resolution lasers.

Accurate treatment of collisional narrowing effects is especially critical in the temperature region around 1000 K. At these temperatures, the first excited vibrational state is weak, and temperature information is contained primarily in the shape of the fundamental band, which is very dependent on collisional narrowing.

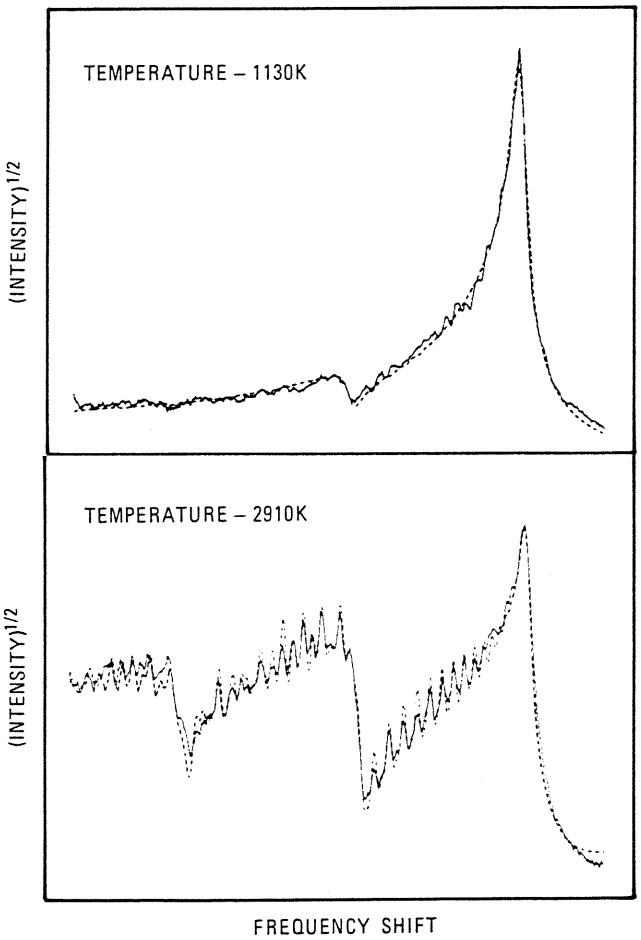

Fig. 7 Typical CARS spectra obtained under knocking conditions. Both the experimental data (solid line) and the theoretical fit (dashed line) are shown a) just prior to the knock point (top); b) and at peak pressure in the post flame gases (bottom).

Typical experimental spectra and the corresponding theoretical fits are shown in Fig. 7. These spectra were averaged over 20 engine cycles and illustrate the spectral dependence on temperature. Several sources of systematic error have been identified from the analysis. Long-term drift in the dye laser spectrum affects temperature accuracy, especially at high temperature, because of the wider frequency range of the Raman signal. Also, the temperature fit at high temperature is very sensitive to the nonresonant background susceptibility. Although the mole fraction of nitrogen in the postflame gases is approximately 0.7, the nonresonant background is not negligible relative to the resonant signal, as would be the case at atmospheric pressure. The combination of the high pressure (29 atm) and high temperature (2900 K) tends to reduce the ratio of resonant to nonresonant signal. Furthermore, the nonresonant susceptibility in the postflame gases is increased over that for pure nitrogen by the presence of significant amounts of water vapor and carbon dioxide.

The estimated accuracy of the averaged CARS temperature measurements is ± 50-75 K. The chief sources of uncertainty in the measurements appear to be dye laser spectral drift and cycle-to-cycle variations in the engine operation.

RESULTS AND DISCUSSION

Using spontaneous Raman scattering from nitrogen, we measured the temperature history in the end gas under both knocking and nonknocking conditions; with CARS, we obtained a limited number of data points under knocking conditions. Figure 8 displays the measured end-gas temperature data. The time interval of these data starts at 2.0 ms before TDC (which is about 6 CAD before TDC) and continues to just beyond the knock point. The solid and dashed lines are smooth curves drawn through the spontaneous Raman knocking and nonknocking data, respectively.

The spontaneous Raman data obtained for knocking operation clearly illustrate the problem of fitting only the unresolved rotational structure of the ground-state vibrational band. At the lower temperatures (600 to 800 K), there is a large amount of scatter that decreases at temperatures above 800 K. This observation is consistent with the fact that above 800 K, the population of the first excited state has become sufficient to influence the accuracy of the temperature determined by the data fit. To reduce this uncertainty, we collected and fit a number of spectra at each point in the cycle so that a more statistically significant temperature could be determined for each point.

The CARS temperature data illustrated in Fig. 8 are in good agreement with the spontaneous Raman data for temperatures above 900 K. At lower temperatures, the agreement is certainly within the limits of the error bounds, however the CARS data may be systematically higher. It is possible that at the lower end-gas temperatures, the pressure may be sufficiently high that the unresolved rotational structure of the ground-state band in spontaneous Raman spectra may be affected by collisional narrowing. The result of not including this effect when fitting spontaneous Raman spectra is a lower predicted temperature. Since collisional narrowing was not included in our analysis of the data, it could certainly be the cause of the small discrepancy in the measurements at these lower temperatures.

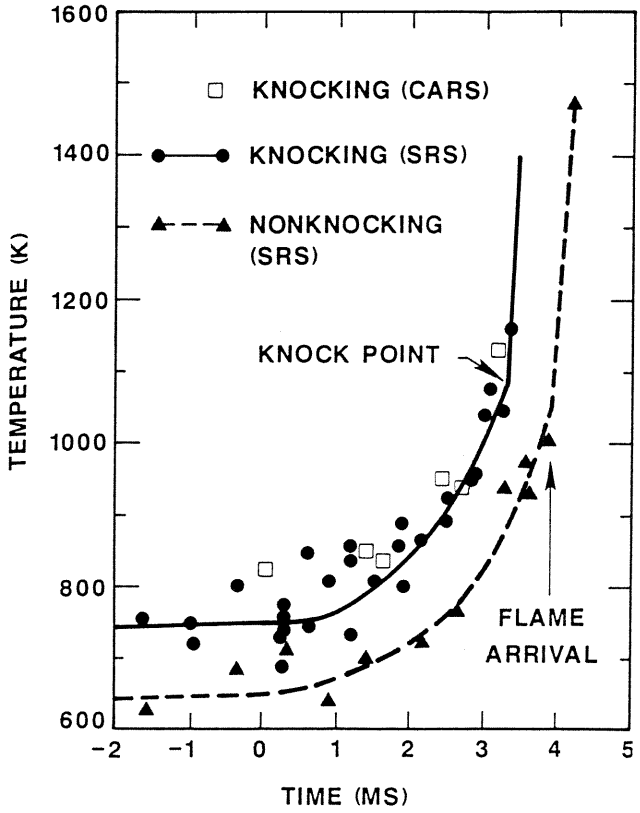

Fig. 8 End gas temperature histories measured using spontaneous Raman scattering (SRS) under knocking and nonknocking conditions, and using CARS, under knocking conditions. The solid and dashed lines are smooth curves drawn through the knocking and nonknocking spontaneous Raman data. The square symbols are the CARS data. Time is measured relative to TDC.

It is interesting to note in Fig. 8 that the end-gas temperature for knocking operation is higher than that for nonknocking operation. Furthermore, the difference of about 100 K is nearly uniform over the time interval of the measurements. We believe that this difference is due to higher wall temperatures under knocking conditions. The weak shock or strong acoustic waves generated by the autoignition will be followed by high local velocities. These high velocities will decrease the thermal boundary layer thickness at the walls and cause an increase in the local heat transfer coefficient. Since this occurs at a time when the bulk gas temperature is highest, the increased heat transfer rates will result in higher wall temperatures.

High wall temperatures can cause an increase in the end-gas temperature through two mechanisms. First, during the intake stroke and early in the compression stroke, when the gas temperature is lower than the wall temperature, higher wall temperatures will result in more heat transferred to the end gas. On the other hand, late in the compression stroke and during the heat release interval, when the end-gas temperature is higher than the wall temperature, there is less heat transferred away from the end gas with the walls at a higher temperature. The net result of both these situations is a higher end gas temperature.

The high wall temperatures also give rise to a primary damage mechanism due to knock. Local surface damage and melting have historically been associated with knock and certainly can be caused by the high wall temperature effects as described above. This is especially true in the region of the spark plug, where the first-burned gases are isentropically heated above their adiabatic flame temperature, aggravating the effects due to knock alone.

CONCLUSIONS

In using the two Raman techniques to measure the end-gas temperatures under knocking conditions, we have come to recognize several important issues. First, the strength of the CARS signal allows a spectrum to be obtained in as little as a single shot of the laser, while the significantly weaker spontaneous Raman technique requires that the signal be averaged over many engine cycles. In addition, at end-gas temperature and pressure conditions, the CARS signal can be detected at a higher resolution because of its signal strength. This yields a more accurate determination of the gas temperature than spontaneous Raman scattering where, at relatively low resolution, we must fit the unresolved rotational structure of a single vibrational band. Furthermore, it appears that at the low temperatures and high pressures characteristic of end-gas conditions, collisional narrowing of the ground-state vibrational band should be considered in the analysis of spontaneous Raman data. Finally, the data fitting process used in both techniques is a complex operation which can, especially in the case of CARS, require a great deal of computational time.

The suitability of a particular technique to a given application must be determined in terms of the required accuracy of the results, the difficulty of obtaining the data and the effort required to process and reduce the data. Indeed, there are other methods such as rotational CARS which could be useful in measuring the end-gas temperature history. The use of this technique is especially interesting at the temperature and pressure conditions prior to end-gas autoignition, since it is not significantly affected by collisional narrowing, and has a strong temperature sensitivity.

ACKNOWLEDGMENTS

This work was funded by the U.S. Department of Energy, Division of Energy Conversion and Utilization Technologies under the management of M. E. Gunn, Jr., and by the Motor Vehicle Manufacturers Association. The CARS measurements were performed in collaboration with Dr. Richard E. Teets of the General Motors Research Laboratories and will be described in detail in a forthcoming article.

REFERENCES

1. Smith, J.R., Green, R.M., Westbrook, C.K. and Pitz, W.J., "An Experimental and Modeling Study of Engine Knock," Twentieth Symposium (International) on Combustion, The Combustion Institute, Pittsburgh, PA, 1984.
2. Rassweiler, G.M. and Withrow, L., "Flame Temperatures Vary with Knock and Combustion-Chamber Position," SAE Trans. 30, 125 (1935)

3. Downs, D., Griffiths, S.T. and Wheeler, R.W., "Pre-flame Reactions in the Spark Ignition Engine: The Influence of Tetraethyl Lead and Other Anti-knocks," J. Inst. Petr., 49, 8 (1963)
4. Alperson, M. and Bradow, R.L., "Investigations into the Composition of End Gases from Otto Cycle Engines," SAE Paper No. 660410, Mid-year Meeting, Detroit, MI (1966)
5. Downs, D., Walsh, A.D. and Wheeler, R.W., "A Study of the Reactions That Lead to 'Knock' in the Spark-Ignition Engine," Phil. Trans. Roy. Soc., A 243, 463 (1951)
6. Pahnke, A.J., Cohen, P.M. and Sturges, B.M., "Pre-flame Oxidation of Hydrocarbons in a Motored Engine," Ind. Engr. Chem. 46, 1024 (1954)
7. Bradow, R.L. and Alperson, M., "Analytical Investigations of Isooctane and Diisobutylene Slow Combustion in an Otto-Cycle Engine," Comb. and Flame 11, 26 (1967)
8. Gluckstein, M.E. and Walcutt C., "End-Gas Temperature-Pressure Histories and Their Relation to Knock," SAE Trans. 69, 529 (1961)
9. Johnson, J.H., Myers, P.S. and Uyehara, O.A., "End-Gas Temperatures, Pressures, Reaction Rates, and Knock," SAE Paper No. 650505, Mid-year Meeting, Chicago Ill. (1965)
10. Johnston, S.C., Robinson, C.W., Rorke, W.S., Smith, J.R. and Witze, P.O., "Application of Laser Diagnostics to an Injected Engine," SAE Trans. 88, 353 (1979)
11. Stephenson, D.A. and Blint, R.J., "The Fitting of Computer Processed Laser Raman Spectra from Methane- and Propane-Air Flames," Appl. Spectrosc., 33, 41 (1979)
12. Green, R.M., Smith, J.R. and Medina, S.C., "Optical Measurements of Hydrocarbons Emitted from a Simulated Crevice Volume in an Engine," SAE Paper No. 840378, International Congress and Exposition, Detroit, MI. (1984)
13. Stenhouse, I.A., Williams, D.R., Cole, J.B. and Swords M.D., "CARS Measurements in an Internal Combustion Engine," Applied Optics 18, 3819 (1979)
14. Klick, D., Marko, K.A. and Rimai, L., "Broadband Single-Pulse CARS Spectra in a Fired Internal Combustion Engine," Applied Optics, 20, 1178 (1981)
15. Kataoka, H., Maeda, S. Hirose, C. and Kajiyama, K., "A Study of N_2 Coherent Anti-Stokes Raman Spectroscopy Thermometry at High Pressure," Appl. Spectrosc., 37, 508 (1983)
16. Rahn, L.A., Johnston, S.C., Farrow, R.L. and Mattern P.L., "CARS Thermometry in an Internal Combustion Engine," in Temperature: Its Measurement and Control in Science and Industry (J.F. Schooley, Ed.), American Institute of Physics, New York, 609 (1982)
17. Alessandretti, G.C. and Violino, P., "Thermometry by CARS in an Automobile Engine," J. Phys. D: Appl. Phys., 16, 1583 (1983)
18. Koszykowski, M.L., Farrow, R.L. and Palmer, R.E., "On the Calculation of Collisionally Narrowed CARS Spectra," Optics Letters, accepted for publication (1985)
19. Hall, R.J., Verdieck, J.F. and Eckbreth, A.C., "Pressure-Induced Narrowing of the CARS Spectrum of N_2," Opt. Comm., 35, 69 (1980)
20. Hall, R.J. and Greenhalgh, D.G., "Application of the Rotational Diffusion Model to Gaseous N_2 CARS Spectra," Opt. Comm., 40, 417 (1982)